

Channel transport: gating, geometry, and heterogeneous diffusion

Sean D. Lawley*

March 17, 2026

Abstract

Channel-mediated transport is ubiquitous in biology. A series of works by different theoreticians have sought to determine how the diffusive flux through a channel depends on (a) stochastic gating, (b) channel geometry, and (c) heterogeneous diffusion. In this paper, we derive an explicit estimate for the diffusive flux through a channel that accounts for these three factors. We show that our estimate is exact in certain parameter regimes. We further use stochastic simulations to confirm that our estimate remains accurate across a very broad range of parameters. Our estimate differs from some results in the physics literature.

Contents

1	Introduction	2
2	Always open channel	5
2.1	Setup	5
2.2	Splitting probability	6
2.3	Two exact equations	8
2.4	Approximation	9
2.5	Approximation is exact as $\min\{\rho_w, \rho_e\} \rightarrow \infty$	9
3	Gated channel	10
3.1	Setup	10
3.2	Splitting probability	11
3.3	Four exact equations	13
3.4	Approximations	14
3.5	Solving the approximate one-dimensional problem	15

*Department of Mathematics, University of Utah, Salt Lake City, UT 84112 USA (lawley@math.utah.edu).

4 Flux asymptotics	16
4.1 Slow switching	17
4.2 Fast switching	17
4.3 Large ρ_e	17
4.4 Large $\min\{\rho_w, \rho_e\}$	17
4.5 Small ρ_w	19
4.6 Short channel	19
4.7 Fast and slow switching in bulks versus channel	20
5 Stochastic simulations	21
5.1 Short channel limit	21
5.2 Variable channel length	21
6 Discussion	22
A Stochastic simulation algorithms	24
A.1 Short channel simulation algorithm	24
A.2 Variable channel length simulations	25

1 Introduction

Diffusive transport through channels or pores is ubiquitous in biology. For example, cells use membrane channels to transport ions between the interior and exterior of the cell [27]. Channels also facilitate transport between subcellular compartments, such as nuclear pores, which mediate exchange between the nucleus and cytoplasm of eukaryotic cells [17]. An example with channels on a larger spatial scale is insect respiration, which relies on diffusive transport of oxygen and carbon dioxide through a network of tracheal tubes [41]. Understanding and quantifying the flux in these and other biological systems is challenging due to three important features:

- (a) stochastic gating,
- (b) channel geometry, and
- (c) different diffusivity inside versus outside the channel.

Elaborating on (a), the channel entrance in many biological systems stochastically opens and closes. In the open state, diffusing “particles” (ions, molecules, proteins, etc.) can freely enter and exit the channel through the gate, whereas the closed state restricts particles from entering or exiting through the gate. See Figure 1 for an illustration. Stochastic gating is often modeled by a two-state Markov jump process,



where $p_0 = 1 - p_1$ denotes the fraction of time that the gate is open and λ parameterizes the overall switching rate between open and closed states.

How does gating affect the flux through the channel? It is often assumed that the average flux through a gated channel, J , is simply the product of the flux through a channel that is always open, J^{open} , and the fraction of time that the gate is open,

$$J = p_0 J^{\text{open}}. \quad (2)$$

Indeed, the simple relation in (2) is a fundamental assumption of the Hodgkin-Huxley model and other conductance-based neuron models [14,15,28]. However, the relation in (2) was challenged in Refs. [18,20], which analyzed a simple model of gated transport in a one-dimensional channel of length L and diffusivity D_c . Refs. [18,20] argued that (2) only holds if the switching rate is much slower than the timescale of diffusion in the channel, i.e. if $\gamma_c := \sqrt{\lambda L^2/D_c} \ll 1$. In fact, Refs. [18,20] argued that the gated flux is identical to the “always open” flux if the switching rate is fast,

$$\lim_{\gamma_c \rightarrow \infty} J = J^{\text{open}}. \quad (3)$$

The prediction in (3) is counterintuitive because it means that even if the gate is open only a small fraction of time ($p_0 \ll 1$), the gated flux can be nearly as high as the flux through a channel that is always open. The counterintuitive prediction in (3) has been contradicted by more recent models and analyses in the physics literature [1–4].

Elaborating on (b), though the flux is understood to be greater through wider and shorter channels, precisely quantifying how channel geometry controls the flux is more difficult. Mathematically, determining this geometric control entails analyzing the diffusion equation in a non-trivial three-dimensional geometry. Indeed, the one-dimensional approximation used in some prior works [18,20] may break down if the channel is not sufficiently narrow.

Elaborating on (c), the particle diffusivity may change upon entering the channel. For example, ATP is thought to diffuse around 10 times slower in voltage-dependent anion channels compared to free solution [31]. Mathematically, such space-dependent diffusivity or “heterogeneous diffusion” introduces multiplicative noise and the associated Itô versus Stratonovich controversy [26] and requires accounting for the so-called “spurious” force associated with any non-Itô interpretation [32,39].

In this paper, we formulate and analyze a model of diffusive transport through a channel that connects two “bulk” reservoirs. See Figure 1 for an illustration. Our main result is an explicit approximation for the average flux through the channel that accounts for (a) stochastic gating, (b) channel geometry, and (c) a diffusivity that is different in the channel versus the bulks. If the channel is a cylinder of radius a and length L and is stochastically gated according to (1), then our estimate of the flux of particles which enter the channel from the “west” (left) bulk and ultimately wander far away into the “east”

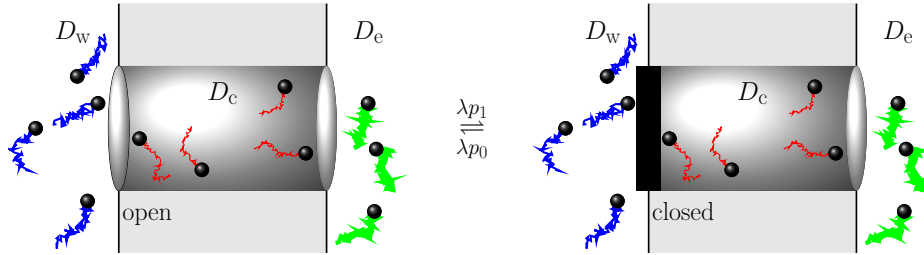


Figure 1: Diffusing particles can pass from the left (or “west”) bulk region through a channel to the right (or “east”) bulk region. Particles have diffusivities D_w , D_c , and D_e in the west bulk, channel, and east bulk. The west entrance to the channel is stochastically gated, which means that it randomly opens and closes. Particles can freely enter and exit the west side of the channel when the gate is open (left diagram), whereas particles can neither enter nor exit through the west side of the channel when the gate is closed (right diagram).

(right) bulk is

$$J_* = 4aD_w c_\infty \mathcal{P}_*, \quad (4)$$

where D_w is the diffusivity in the west bulk, c_∞ is the fixed particle concentration far away in the west bulk, and

$$\mathcal{P}_* = \left[\frac{4\rho_w}{\pi} \left(1 + \frac{p_1}{p_0} \frac{\tanh(\gamma_c)}{\gamma_c} + \frac{\pi}{4\rho_e} + \frac{(p_1/p_0)\text{sech}^2(\gamma_c)}{\rho_e(\frac{4}{\pi} + \gamma_e) + \gamma_c \tanh(\gamma_c)} \right) + \frac{\frac{4}{\pi} + \gamma_w p_0}{\frac{4}{\pi} p_0 + \gamma_w p_0} \right]^{-1},$$

which is the probability that a particle which reaches the west entrance to the channel from far away in the west bulk will eventually traverse the channel and wander far away into east bulk. The probability \mathcal{P}_* is a function of the fraction of time that the gate is open, $p_0 = 1 - p_1$, the following three dimensionless parameters,

$$\gamma_w = \sqrt{\frac{\lambda a^2}{D_w}}, \quad \gamma_c = \sqrt{\frac{\lambda L^2}{D_c}}, \quad \gamma_e = \sqrt{\frac{\lambda a^2}{D_e}},$$

which compare the switching rate λ to the diffusion timescales in the west bulk, channel, and east bulk (where D_c and D_e are the respective diffusivities in the channel and east bulk), and the following two dimensionless parameters,

$$\rho_w = \frac{L}{a} \left(\frac{D_w}{D_c} \right)^{\alpha_w}, \quad \rho_e = \frac{L}{a} \left(\frac{D_e}{D_c} \right)^{\alpha_e},$$

which compare the channel aspect ratio L/a to the change in diffusivity at the west and east channel entrances, where $\alpha_w \in [0, 1]$ and $\alpha_e \in [0, 1]$ specify the interpretation of the multiplicative noise (where the values $\alpha = 0$, $\alpha = 1/2$, and $\alpha = 1$ correspond respectively to the Itô [16], Stratonovich [35], and kinetic

interpretations [13]). We derive (4) by analyzing a system of reaction-diffusion equations in three spatial dimensions. We also generalize (4) to channels with more general cross-sectional shapes.

We show that our flux estimate J_* in (4) is exact if $\min\{\rho_w, \rho_e\} \gg 1$ in the sense that

$$J_*/J_{\text{exact}} \rightarrow 1 \quad \text{as } \min\{\rho_w, \rho_e\} \rightarrow \infty, \quad (5)$$

where J_{exact} is the exact flux (which is not known explicitly). We further use stochastic simulations to show that J_* is accurate in a very broad range of parameters,

$$J_* \approx J_{\text{exact}}.$$

Indeed, we have been unable to find a parameter regime in which J_* is inaccurate. We also show that J_* reduces to some prior flux estimates [18, 20, 22] in certain special cases and that J_* satisfies the counterintuitive relation for fast switching in (3) if we take $\min\{\gamma_w, \gamma_c, \gamma_e\} \rightarrow \infty$. We show that J_* differs from some prior flux estimates derived in the physics literature [1–3].

The rest of the paper is organized as follows. We start in section 2 by deriving the following flux estimate for the case that the channel is always open,

$$J_*^{\text{open}} = 4aD_w c_\infty \mathcal{P}_*^{\text{open}}, \quad \text{where } \mathcal{P}_*^{\text{open}} = \frac{1}{1 + \rho_w/\rho_e + (4/\pi)\rho_w}.$$

We then consider a gated channel in section 3 and derive J_* in (4). Section 4 explores the behavior of J_* in various asymptotic regimes, including showing that J_* is exact in the sense of (5). Section 5 compares J_* to stochastic simulations. We conclude in section 6 by discussing related work, including discrepancies between J_* and prior estimates.

2 Always open channel

2.1 Setup

Consider a particle diffusing in an unbounded, three-dimensional domain given by the union $\Omega_w \cup \Omega_c \cup \Omega_e \subset \mathbb{R}^3$, where the left bulk, channel, and right bulk are the following three respective sets,

$$\begin{aligned} \Omega_w &= \{(x, y, z) \in \mathbb{R}^3 : x < -L/2\}, \\ \Omega_c &= \{(x, y, z) \in \mathbb{R}^3 : x \in (-L/2, L/2), (y, z) \in a\Gamma\}, \\ \Omega_e &= \{(x, y, z) \in \mathbb{R}^3 : x > L/2\}. \end{aligned}$$

The subscripts “w,” “c,” and “e” are for “west,” “channel” (or “central”), and “east.” The channel Ω_c has length $L > 0$, diameter $\mathcal{O}(a)$, and cross-sectional shape $a\Gamma \subset \mathbb{R}^2$, where $\Gamma \subset \mathbb{R}^2$ is a dimensionless shape with on order one diameter $\text{diam}(\Gamma) = \mathcal{O}(1)$ (recall that the diameter of a set is the maximum

possible distance between any two points in that set). We are most interested in the case that the channel is a cylinder of radius a (in which case Γ is the unit disk), but we proceed in terms of a general cross-sectional shape.

Suppose that the diffusivity is the following piecewise constant function of the x coordinate,

$$D(x, y, z) = D(x) = \begin{cases} D_w & \text{if } x < -L/2, \\ D_c & \text{if } x \in (-L/2, L/2), \\ D_e & \text{if } x > L/2. \end{cases} \quad (6)$$

To specify the interpretation of the multiplicative noise (inherent to any space-dependent diffusivity [26,34,37–40]), suppose that the probability density $p(x, y, z, t)$ that the particle is at position (x, y, z) at time t satisfies the following continuity conditions at the west channel entrance,

$$\begin{aligned} D_w^{1-\alpha_w} p(-L/2^-, y, z, t) &= D_c^{1-\alpha_w} p(-L/2^+, y, z, t), & (y, z) \in a\Gamma, \\ D_w \partial_x p(-L/2^-, y, z, t) &= D_c \partial_x p(-L/2^+, y, z, t), & (y, z) \in a\Gamma, \end{aligned}$$

and analogous conditions at the east channel entrance,

$$\begin{aligned} D_c^{1-\alpha_e} p(L/2^-, y, z, t) &= D_e^{1-\alpha_e} p(L/2^+, y, z, t), & (y, z) \in a\Gamma, \\ D_c \partial_x p(L/2^-, y, z, t) &= D_e \partial_x p(L/2^+, y, z, t), & (y, z) \in a\Gamma, \end{aligned}$$

where $g(x_0^\pm) = \lim_{x \rightarrow x_0^\pm} g(x)$ denotes one-sided limits. The parameters $\alpha_w \in [0, 1]$ and $\alpha_e \in [0, 1]$ specify the interpretation of the multiplicative noise [10], with the most common [26] interpretations being $\alpha = 0$ (Itô [16]) and $\alpha = 1/2$ (Stratonovich [35]). Another convention is $\alpha = 1$, which is sometimes called kinetic, isothermal, or Hänggi-Klimontovich [13].

The flux J of particles which enter the channel from the west bulk and ultimately wander far into the east bulk is the product of (i) the flux of particles from the west bulk which reach the west entrance to the channel at $x = -L/2$, and (ii) the probability \mathcal{P} that a particle which arrives at the west channel entrance from the west bulk will eventually wander far into the east bulk and never return to the channel. That is, the flux J is given by

$$J = (2\pi C_0(\Gamma) a D_w c_\infty) \mathcal{P}, \quad (7)$$

where $C_0(\Gamma)$ is the electrostatic capacitance of Γ (capacitance is defined so that the capacitance of a unit disk is $2/\pi$). The geometric prefactor $2\pi C_0(\Gamma) a$ can be derived via a simple divergence theorem argument [23]. Note that $2\pi C_0(\Gamma) a = 4a$ for a cylindrical channel [5].

2.2 Splitting probability

Suppose that the stochastic gate is always open. Let $P^{\text{open}}(\mathbf{x}) = P(\mathbf{x})$ be the probability that a particle that starts at $\mathbf{x} = (x, y, z)$ will eventually wander far

away into the east bulk and never return to the channel,

$$P(\mathbf{x}) := \mathbb{P}\left(\limsup_{t \rightarrow \infty} X(t) \geq L/2 \mid \mathbf{X}(0) = \mathbf{x}\right),$$

where $(X(t), Y(t), Z(t))$ denotes the stochastic position of the particle at time t . The function P is harmonic in the two bulks and in the channel,

$$\Delta P = 0, \quad \mathbf{x} \in \Omega_w \cup \Omega_c \cup \Omega_e, \quad (8)$$

satisfies the far-field conditions,

$$\lim_{\|\mathbf{x}\| \rightarrow \infty, x < -L/2} P(\mathbf{x}) = 0, \quad \lim_{\|\mathbf{x}\| \rightarrow \infty, x > L/2} P(\mathbf{x}) = 1,$$

continuity conditions at $x = -L/2$,

$$P(-L/2^-, y, z) = P(-L/2^+, y, z) \quad (y, z) \in a\Gamma, \quad (9)$$

$$D_w^{\alpha_w} \partial_x P(-L/2^-, y, z) = D_c^{\alpha_w} \partial_x P(-L/2^+, y, z) \quad (y, z) \in a\Gamma, \quad (10)$$

and analogous continuity conditions at $x = L/2$,

$$P(L/2^-, y, z) = P(L/2^+, y, z) \quad (y, z) \in a\Gamma, \quad (11)$$

$$D_c^{\alpha_e} \partial_x P(L/2^-, y, z) = D_e^{\alpha_e} \partial_x P(L/2^+, y, z) \quad (y, z) \in a\Gamma,$$

and satisfies reflecting boundary conditions on the rest of the boundary of $\Omega_w \cup \Omega_c \cup \Omega_b$.

For a particle which reaches the west channel entrance from far away in the west bulk, the probability of wandering far into the east bulk is

$$\mathcal{P}(-L/2) := \int_{a\Gamma} P(-L/2, y, z) \mu(y, z) dy dz, \quad (12)$$

where $\mu(y, z)$ is the probability density of where the particle hits the channel entrance if it started far from the channel and is conditioned to hit the channel. That is, $\mu(y, z)$ is the so-called harmonic measure density [12]. If the channel is a cylinder of radius a , then μ has a density given by the following explicit function [33] of the radius $r = \sqrt{y^2 + z^2} \in [0, a)$,

$$\mu(r) = \frac{r}{2\pi a^2 \sqrt{1 - (r/a)^2}}, \quad r^2 = y^2 + z^2 < a^2. \quad (13)$$

Let \bar{P} denote the uniform average of P in the channel cross-section,

$$\bar{P}(x) := \frac{1}{|a\Gamma|} \int_{a\Gamma} P(x, y, z) dy dz, \quad (14)$$

where $|a\Gamma| = a^2|\Gamma|$ denotes the area of the channel cross-section. Integrating (8), using the two-dimensional divergence theorem and the reflecting boundary conditions, and solving the resulting ordinary differential equations yields that $\bar{P}(x)$ is the following linear function,

$$\bar{P}(x) = \bar{P}(-L/2) + (x/L)(\bar{P}(L/2) - \bar{P}(-L/2)).$$

Taking the derivative yields

$$\bar{P}'(-L/2^+) = (\bar{P}(L/2) - \bar{P}(-L/2))/L > 0. \quad (15)$$

2.3 Two exact equations

We now derive two exact equations involving the four probabilities $\mathcal{P}(\pm L/2)$ and $\bar{\mathcal{P}}(\pm L/2)$. Integrating (8) over a large hemisphere H_R of radius $R \gg a$ in the left bulk,

$$H_R = \{(x, y, z) \in \mathbb{R}^3 : x < -L/2, (x + L/2)^2 + y^2 + z^2 < R^2\}, \quad (16)$$

and using the divergence theorem yields

$$0 = \int_{H_R} \Delta P \, d\mathbf{x} = \int_{\partial H_R^+} \partial_{\mathbf{n}} P \, dS + \int_{a\Gamma} \partial_x P(-L/2^-, y, z) \, dy \, dz, \quad (17)$$

where $\partial_{\mathbf{n}}$ denotes the normal derivative and ∂H_R^+ denotes the curved part of the boundary of the hemisphere H_R ,

$$\partial H_R^+ = \{(x, y, z) \in \mathbb{R}^3 : x < -L/2, (x + L/2)^2 + y^2 + z^2 = R^2\}. \quad (18)$$

The strong Markov property implies that P has the following monopole decay at far-field [23],

$$P(\mathbf{x}) \sim \frac{C_0(a\Gamma)\mathcal{P}(-L/2)}{\|\mathbf{x}\|} \quad \text{as } \|\mathbf{x}\| \rightarrow \infty, \quad x < -L/2,$$

and therefore

$$\int_{\partial H_R^+} \partial_{\mathbf{n}} P \, dS \rightarrow -2\pi a C_0(\Gamma)\mathcal{P}(-L/2) < 0 \quad \text{as } R \rightarrow \infty.$$

Furthermore, the second continuity condition in (9) and the derivative of \bar{P} in (15) imply

$$\begin{aligned} \int_{a\Gamma} \partial_x P(-L/2^-, y, z) \, dy \, dz &= \left(\frac{D_c}{D_w}\right)^{\alpha_w} \int_{a\Gamma} \partial_x P(-L/2^+, y, z) \, dy \, dz \\ &= \left(\frac{D_c}{D_w}\right)^{\alpha_w} |\Gamma| a \frac{a}{L} (\bar{P}(L/2) - \bar{P}(-L/2)). \end{aligned}$$

Therefore,

$$\mathcal{P}(-L/2) = \frac{1}{G(\Gamma)} \frac{(\bar{P}(L/2) - \bar{P}(-L/2))}{\rho_w}, \quad (19)$$

where $G(\Gamma)$ is the following dimensionless geometric factor,

$$G(\Gamma) = \frac{2\pi C_0(\Gamma)}{|\Gamma|} > 0, \quad (20)$$

and ρ_w is the following dimensionless comparison of the tube aspect ratio and the change of diffusivity at the west channel entrance,

$$\rho_w := (L/a)(D_w/D_c)^{\alpha_w} > 0. \quad (21)$$

Note that the geometric factor in (20) is $G(\Gamma) = 4/\pi$ if the tube is a cylinder (i.e. if Γ is the unit disk).

By symmetry, we obtain the analog of (19) at the east channel entrance,

$$1 - \mathcal{P}(L/2) = \frac{1}{G(\Gamma)} \frac{(\bar{P}(L/2) - \bar{P}(-L/2))}{\rho_e}, \quad (22)$$

where $\mathcal{P}(L/2)$ is defined analogously to (12),

$$\mathcal{P}(L/2) := \int_{a\Gamma} P(L, y, z) \mu(y, z) dy dz,$$

and ρ_e is defined analogously to (21),

$$\rho_e := (L/a)(D_e/D_c)^{\alpha_e} > 0.$$

We emphasize that (19) and (22) are exact relations.

2.4 Approximation

To obtain an explicit approximation from the exact relations (19) and (22), we ignore variation in the channel cross-section and make the approximations

$$\mathcal{P}(-L/2) \approx \bar{P}(-L/2), \quad \mathcal{P}(L/2) \approx \bar{P}(L/2), \quad (23)$$

so that (19) and (22) becomes a linear system in the two variables $\mathcal{P}(\pm L/2)$, which we solve to obtain the approximation

$$\mathcal{P}(-L/2) \approx \mathcal{P}_*^{\text{open}} := \frac{1}{1 + \rho_w/\rho_e + G(\Gamma)\rho_w}, \quad (24)$$

where the superscript “open” emphasizes that (24) is for the case that the channel is always open. The formula (24) generalizes a result of Ref. [23] to the case that the diffusivities in the two bulks may differ.

We show below that the approximation (24) is exact if $\rho_w \gg 1$ and $\rho_e \gg 1$. We note that if $\rho_w = \rho_e = \rho$ (which happens if $D_w = D_e$ and $\alpha_w = \alpha_e$ or $\alpha_w = \alpha_e = 0$), then it was shown in Ref. 23 using stochastic simulations that (24) is accurate for all $\rho > 0$ in the case of a cylindrical channel. We further note that $\lim_{\rho_e \rightarrow \infty} \mathcal{P}_*^{\text{open}} = 1/(1 + G(\Gamma)\rho_w)$, which was an approximation derived in Ref. 30 for the probability of merely reaching the east end of the tube (rather than reaching the east end of the tube and then wandering far away into the east bulk).

2.5 Approximation is exact as $\min\{\rho_w, \rho_e\} \rightarrow \infty$

We claim that the approximation $\mathcal{P}_*^{\text{open}}$ in (24) is exact if $\rho_w \gg 1$ and $\rho_e \gg 1$. That is, we claim

$$\mathcal{P}(-L/2) \sim \frac{1}{G(\Gamma)\rho_w} \sim \mathcal{P}_*^{\text{open}} \quad \text{as } \min\{\rho_w, \rho_e\} \rightarrow \infty, \quad (25)$$

where $f \sim g$ means $f/g \rightarrow 1$. We need only show the first asymptotic equivalence in (25), since the second asymptotic equivalence in (25) is immediate from (24) (we assume throughout this paper that $G(\Gamma) = \mathcal{O}(1)$; note that $G(\Gamma) = 4/\pi \approx 1.27$ if the channel is a cylinder). The first asymptotic equivalence in (25) follows from the exact relation in (19) if we can show that

$$\lim_{\rho_w \rightarrow \infty} \bar{P}(-L/2) = 0, \quad (26)$$

$$\lim_{\rho_e \rightarrow \infty} \bar{P}(L/2) = 1. \quad (27)$$

By the strong Markov property,

$$\bar{P}(-L/2) \leq \bar{u}(-L/2), \quad (28)$$

where $\bar{u}(x) = \frac{1}{a^2|\Gamma|} \int_{a\Gamma} u(x, y, z) dy dz$ and $u(x, y, z)$ is the probability that the diffusing particle will reach the east end of the channel given that it started at (x, y, z) . The limit $\lim_{\rho_w \rightarrow \infty} \bar{u}(-L/2) = 0$ was shown in Ref. [30], and thus (28) implies (26). The result (27) holds by symmetry.

3 Gated channel

3.1 Setup

Consider the model of section 2, but suppose that there is a stochastic gate at the west channel entrance that opens and closes according to the Markov jump process,

$$\text{open} \quad 0 \xrightleftharpoons[\lambda_1]{\lambda_0} 1 \quad \text{closed}, \quad (29)$$

where the opening and closing rates are

$$\begin{aligned} \lambda_1 &= p_0 \lambda \quad (\text{opening rate}), \\ \lambda_0 &= p_1 \lambda \quad (\text{closing rate}), \end{aligned} \quad (30)$$

and p_0 and $p_1 = 1 - p_0$ are the steady-state probabilities of the gate being open and closed,

$$\begin{aligned} p_0 &= \frac{\lambda_1}{\lambda_0 + \lambda_1} \quad (\text{probability open}), \\ p_1 &= \frac{\lambda_0}{\lambda_0 + \lambda_1} \quad (\text{probability closed}), \end{aligned} \quad (31)$$

and $\lambda = \lambda_0 + \lambda_1$ parameterizes the “switching rate” between the open and closed states.

3.2 Splitting probability

Let $P_0(\mathbf{x})$ (respectively, $P_1(\mathbf{x})$) be the probability that a particle that starts at position $\mathbf{x} = (x, y, z)$ will eventually wander far into the east bulk and never return to the channel, given that the gate is initially open (respectively, closed). These probabilities satisfy the following Kolmogorov backward equations,

$$\begin{aligned} 0 &= D(x)\Delta P_0 - \lambda_0(P_0 - P_1), \\ 0 &= D(x)\Delta P_1 - \lambda_1(P_1 - P_0), \end{aligned} \tag{32}$$

where $D(x)$ is in (6), with far-field conditions,

$$\begin{aligned} \lim_{\|\mathbf{x}\| \rightarrow \infty, x < -L/2} P_0(\mathbf{x}) &= \lim_{\|\mathbf{x}\| \rightarrow \infty, x < -L/2} P_1(\mathbf{x}) = 0, \\ \lim_{\|\mathbf{x}\| \rightarrow \infty, x > L/2} P_0(\mathbf{x}) &= \lim_{\|\mathbf{x}\| \rightarrow \infty, x > L/2} P_1(\mathbf{x}) = 1. \end{aligned}$$

At the west entrance to the channel, P_0 satisfies the continuity conditions in (9) and P_1 satisfies no flux conditions,

$$\partial_x P_1(-L/2^-, y, z) = \partial_x P_1(L/2^+, y, z) = 0, \quad (y, z) \in a\Gamma. \tag{33}$$

At the east entrance to the channel, P_0 and P_1 satisfy the continuity conditions in (11).

Diagonalize (32) by introducing

$$P = p_0 P_0 + p_1 P_1, \tag{34}$$

$$Q = P_0 - P_1, \tag{35}$$

so that P and Q satisfy the following decoupled partial differential equations,

$$\Delta P = 0, \tag{36}$$

$$D(x)\Delta Q = \lambda Q. \tag{37}$$

Furthermore, P and Q satisfy the far-field conditions,

$$\begin{aligned} \lim_{\|\mathbf{x}\| \rightarrow \infty, x < -L/2} P(\mathbf{x}) &= \lim_{\|\mathbf{x}\| \rightarrow \infty, x < -L/2} Q(\mathbf{x}) = 0, \\ \lim_{\|\mathbf{x}\| \rightarrow \infty, x > L/2} P(\mathbf{x}) &= 1, \quad \lim_{\|\mathbf{x}\| \rightarrow \infty, x > L/2} Q(\mathbf{x}) = 0, \end{aligned}$$

and P and Q satisfy the continuity conditions at the east end of the channel in (11). The functions P and Q are decoupled, except for their conditions at the west end of the channel, which can be derived from the fact that P_0 satisfies (9), P_1 satisfies (33), and the following representations (which are equivalent to (34)-(35)),

$$\begin{aligned} P_0 &= P + p_1 Q, \\ P_1 &= P - p_0 Q. \end{aligned}$$

If a particle arrives at the west entrance to the channel from far away in the west bulk, then the gate will be in its stationary distribution (p_0 and p_1 in (31)), and thus

$$\mathcal{P}(-L/2^-) = p_0\mathcal{P}_0(-L/2) + p_1\mathcal{P}_1(-L/2^-), \quad (38)$$

where

$$\mathcal{P}_0(-L/2) = \int_{a\Gamma} P_0(-L/2, y, z) \mu(y, z) dy dz, \quad (39)$$

$$\mathcal{P}_1(-L/2^-) = \int_{a\Gamma} P_1(-L/2^-, y, z) \mu(y, z) dy dz, \quad (40)$$

and μ is the harmonic measure density in (12). We emphasize that P_1 is evaluated at $x = -L/2^-$ in the definition of $\mathcal{P}_1(-L/2^-)$. We further define

$$\mathcal{P}(L/2) = p_0\mathcal{P}_0(L/2) + p_1\mathcal{P}_1(L/2),$$

where

$$\mathcal{P}_i(L/2) = \int_{a\Gamma} P_i(L/2, y, z) \mu(y, z) dy dz, \quad i \in \{0, 1\}.$$

Define

$$\bar{P}_i(x) := \frac{1}{|a\Gamma|} \int_{a\Gamma} P_i(x, y, z) dy dz, \quad i \in \{0, 1\},$$

and $\bar{P}(x) = p_0\bar{P}_0(x) + p_1\bar{P}_1(x)$ and $\bar{Q}(x) = \bar{P}_0(x) - \bar{P}_1(x)$. Hence, integrating (32), using the two-dimensional divergence theorem and the reflecting boundary conditions, we find that \bar{P}_0 and \bar{P}_1 satisfy the backward Kolmogorov equations (32) (which are now ordinary differential equations in the single variable x) with boundary condition

$$\bar{P}'_1(-L/2^+) = \bar{P}'(-L/2^+) - p_0\bar{Q}'(-L/2^+) = 0. \quad (41)$$

Therefore, we obtain $\bar{P}(x)$ and $\bar{Q}(x)$ (and therefore $\bar{P}_0(x)$ and $\bar{P}_1(x)$) as the following explicit functions of the three unknowns $\bar{P}(-L/2^+)$, $\bar{P}(L/2)$, and $\bar{Q}(L/2)$,

$$\begin{aligned} \bar{P}(x) &= \frac{x(\bar{P}(L/2) - \bar{P}(-L/2^+))}{L} + \frac{\bar{P}(-L/2^+) + \bar{P}(L/2)}{2}, \quad x \in (-L/2, L/2], \\ \bar{Q}(x) &= \operatorname{sech}(\gamma_c) \left[\frac{(\bar{P}(-L/2^+) - \bar{P}(L/2)) \sinh\left(\frac{\gamma_c(L-2x)}{2L}\right)}{\gamma_c p_0} \right. \\ &\quad \left. + \bar{Q}(L/2) \cosh\left(\gamma_c\left(\frac{x}{L} + \frac{1}{2}\right)\right) \right] \quad x \in (-L/2, L/2], \end{aligned} \quad (42)$$

where $\gamma_c = \sqrt{\lambda L^2/D_c}$ compares the switching rate to the timescale of diffusion in the channel.

3.3 Four exact equations

We now derive four exact equations involving the eight probabilities $\mathcal{P}_0(\pm L/2)$, $\mathcal{P}_1(\pm L/2)$, $\bar{\mathcal{P}}_0(\pm L/2)$, and $\bar{\mathcal{P}}_1(\pm L/2)$. Integrating (36) over the hemisphere H_R in (16) in the west bulk and using the divergence theorem yields

$$0 = \int_{H_R} \Delta P \, d\mathbf{x} = \int_{\partial H_R^+} \partial_{\mathbf{n}} P \, dS + \int_{a\Gamma} \partial_x P(-L/2^-, y, z) \, dy \, dz,$$

where ∂H_R^+ denotes the curved part of the boundary of the hemisphere H_R in (18). The strong Markov property implies that P has the following monopole decay at far-field [23],

$$P(\mathbf{x}) \sim \frac{C_0(a\Gamma)\mathcal{P}(-L/2^-)}{\|\mathbf{x}\|} \quad \text{as } \|\mathbf{x}\| \rightarrow \infty, \, x < -L/2,$$

and therefore

$$\int_{\partial H_R^+} \partial_{\mathbf{n}} P \, dS \rightarrow -2\pi a C_0(\Gamma)\mathcal{P}(-L/2^-) < 0 \quad \text{as } R \rightarrow \infty.$$

Furthermore, the second continuity condition in (9) implies

$$\begin{aligned} \int_{a\Gamma} \partial_x P(-L/2^-, y, z) \, dy \, dz &= p_0 \int_{a\Gamma} \partial_x P_0(-L/2^-, y, z) \, dy \, dz \\ &= p_0 \left(\frac{D_c}{D_w} \right)^{\alpha_w} \int_{a\Gamma} \partial_x P_0(-L/2^+, y, z) \, dy \, dz \\ &= p_0 \left(\frac{D_c}{D_w} \right)^{\alpha_w} |\Gamma| a \frac{a}{L} L \bar{\mathcal{P}}'_0(-L/2^+). \end{aligned}$$

Therefore, we have the following exact equation,

$$\rho_w G(\Gamma)\mathcal{P}(-L/2^-) = p_0 L \bar{\mathcal{P}}'_0(-L/2^+) = L \bar{\mathcal{P}}'(-L/2^+). \quad (43)$$

Similarly, integrating (37) in the west bulk and using the divergence theorem yields

$$\begin{aligned} 0 &= \lambda/D_w \int_{x < -L/2} Q \, d\mathbf{x} - \int_{a\Gamma} \partial_x Q(L/2^-, y, z) \, dy \, dz \\ &= \lambda/D_w \int_{x < -L/2} Q \, d\mathbf{x} - \int_{a\Gamma} \partial_x P_0(L/2^-, y, z) \, dy \, dz \\ &= \lambda/D_w \int_{x < -L/2} Q \, d\mathbf{x} - \frac{2a\pi C_0(\Gamma)\mathcal{P}(-L/2^-)}{p_0}, \end{aligned}$$

and therefore we obtain the exact equation,

$$G(\Gamma)\mathcal{P}(-L/2^-) = p_0 \frac{\lambda}{D_w} \frac{1}{a} \frac{1}{|\Gamma|} \int_{x < -L/2} Q \, d\mathbf{x} = p_0 (\gamma_w)^2 \frac{1}{a} \frac{1}{a^2 |\Gamma|} \int_{x < -L/2} Q \, d\mathbf{x}, \quad (44)$$

where $\gamma_w = \sqrt{\lambda a^2/D_w}$ and $\int_{x < -L/2} Q \, d\mathbf{x}$ denotes the volume integral of $Q(x, y, z)$ over the entire west bulk.

Integrating (36) in the east bulk and using the divergence theorem, the far-field behavior, and the continuity conditions in (11) yields

$$\begin{aligned} 0 &= -2\pi a C_0(\Gamma)(1 - \mathcal{P}(L/2)) + \int_{a\Gamma} \partial_x P(L/2^+, y, z) \, dy \, dz \\ &= -2\pi a C_0(\Gamma)(1 - \mathcal{P}(L/2)) + \left(\frac{D_c}{D_e}\right)^{\alpha_e} \int_{a\Gamma} \partial_x P(L/2^-, y, z) \, dy \, dz, \end{aligned}$$

and therefore we have the following exact equation,

$$L\bar{P}'(L/2^-) = G(\Gamma)\rho_e(1 - \mathcal{P}(L/2)). \quad (45)$$

Similarly, integrating (37) and using the divergence theorem and the continuity conditions in (11) yields

$$\begin{aligned} 0 &= \lambda/D_e \int_{x > L/2} Q \, d\mathbf{x} + \int_{a\Gamma} \partial_x Q(L/2^+, y, z) \, dy \, dz \\ &= \lambda/D_e \int_{x > L/2} Q \, d\mathbf{x} + \left(\frac{D_c}{D_e}\right)^{\alpha_e} \int_{a\Gamma} \partial_x Q(L/2^-, y, z) \, dy \, dz, \end{aligned}$$

and therefore we have the exact equation,

$$L\bar{Q}'(L/2^-) = \frac{-\lambda\rho_e}{D_e} \frac{1}{a|\Gamma|} \int_{x > L/2} Q \, d\mathbf{x} = -\rho_e(\gamma_e)^2 \frac{1}{a} \frac{1}{a^2|\Gamma|} \int_{x > L/2} Q \, d\mathbf{x}, \quad (46)$$

where $\gamma_e = \sqrt{\lambda a^2/D_e}$.

3.4 Approximations

We now posit some approximations to turn the four exact equations in (43), (44), (45), and (46) into four approximate equations which will yield explicit estimates of the three quantities $\bar{P}(-L/2^+)$, $\bar{P}(L/2)$, and $\bar{Q}(L/2)$ in (42) and the fourth quantity $\mathcal{P}(-L/2^-)$ in (38). The approximations at $x = -L/2$ are

$$\mathcal{P}_0(-L/2) \approx \bar{P}_0(-L/2), \quad (47)$$

$$\mathcal{P}_1(-L/2^-) \approx \bar{P}_1(-L/2^-), \quad (48)$$

$$(\gamma_w)^2 \frac{1}{a} \frac{1}{a^2|\Gamma|} \int_{x < -L/2} Q \, d\mathbf{x} \approx (G(\Gamma) + \gamma_w)\bar{Q}(-L/2^-), \quad (49)$$

and the analogous approximations at $x = L/2$ are

$$\mathcal{P}_0(L/2) \approx \bar{P}_0(L/2), \quad (50)$$

$$\mathcal{P}_1(L/2) \approx \bar{P}_1(L/2), \quad (51)$$

$$(\gamma_e)^2 \frac{1}{a} \frac{1}{a^2|\Gamma|} \int_{x > L/2} Q \, d\mathbf{x} \approx (G(\Gamma) + \gamma_e)\bar{Q}(L/2). \quad (52)$$

The approximations in (47)-(48) and (50)-(51) ignore variation in the channel cross-section (analogous to (23)). The approximations in (49) and (52) ignore variation in the channel cross-section and further use a simple approximation to the modified Helmholtz equation in (37) which is valid for both small and large λ (derived in Appendix B of Ref. 22).

Combining the approximation (49) with the exact equation (44) yields

$$G(\Gamma)\mathcal{P}(-L/2^-) \approx p_0(G(\Gamma) + \gamma_w)\bar{Q}(-L/2^-). \quad (53)$$

Rearranging (53) and using (47)-(48) yields

$$\mathcal{P}_1(-L/2^-) \approx \frac{p_0\gamma_b}{G(\Gamma) + p_0\gamma_b}\mathcal{P}_0(-L/2), \quad (54)$$

which is equivalent to

$$\mathcal{P}(-L/2^-) \approx \frac{1}{1 + \frac{p_1}{p_0}\frac{G(\Gamma)}{G(\Gamma) + \gamma_w}}\mathcal{P}_0(-L/2) = \left(p_0 + \frac{p_1 p_0 \gamma_w}{G(\Gamma) + p_0 \gamma_w}\right)\mathcal{P}_0(-L/2). \quad (55)$$

Hence, if we use the approximations (47)-(48) and (54), then the exact equation in (43) becomes the following approximate boundary condition,

$$L\bar{P}'_0(-L/2^+) \approx \rho_w G(\Gamma) \left(1 + \frac{p_1 \gamma_w}{G(\Gamma) + p_0 \gamma_w}\right) \bar{P}_0(-L/2). \quad (56)$$

Furthermore, combining the approximations (50)-(51) with the exact equation (45) yields the following approximate boundary condition,

$$L\bar{P}'(L/2^-) \approx G(\Gamma)\rho_e(1 - \bar{P}(L/2)). \quad (57)$$

Finally, combining the approximation in (52) with the exact equation (46) yields the following approximate boundary condition,

$$L\bar{Q}'(L/2^-) \approx -\rho_e(G(\Gamma) + \gamma_e)\bar{Q}(L/2). \quad (58)$$

3.5 Solving the approximate one-dimensional problem

If we treat the three approximate boundary conditions in (56), (57), and (58) as equalities, then we obtain the following boundary value problem for $\hat{P}(x)$ and $\hat{Q}(x)$ which approximate $\bar{P}(x)$ and $\bar{Q}(x)$,

$$\begin{aligned} \hat{P}'' &= 0, & x &\in (-L/2, L/2), \\ \hat{Q}'' &= (\lambda/D_c)\hat{Q}, & x &\in (-L/2, L/2), \\ \hat{P}' &= p_0\hat{Q}', & x &= -L/2^+, \\ L(\hat{P} + p_1\hat{Q})' &= \rho_w G(\Gamma) \left(1 + \frac{p_1 \gamma_w}{G(\Gamma) + p_0 \gamma_w}\right) (\hat{P} + p_1\hat{Q}), & x &= -L/2^+, \\ L\hat{P}' &= \rho_e G(\Gamma)(1 - \hat{P}), & x &= L/2^-, \\ L\hat{Q}' &= -\rho_e(G(\Gamma) + \gamma_e)\hat{Q} & x &= L/2^-, \end{aligned}$$

where the first boundary condition is the exact boundary condition in (41). It is straightforward to solve this boundary value problem and obtain explicit formulas for $\hat{P}(x)$ and $\hat{Q}(x)$. For brevity, we omit these complicated formulas.

For our purposes, we are primarily interested in the following explicit approximation to $\mathcal{P}(-L/2^-)$ obtained from $\hat{P}_0(-L/2) = \hat{P}(-L/2^+) + p_1 \hat{Q}(-L/2^+)$ and (55),

$$\begin{aligned} \mathcal{P}(-L/2^-) &\approx \mathcal{P}_* := \left(p_0 + \frac{p_1 p_0 \gamma_w}{G(\Gamma) + p_0 \gamma_w} \right) \hat{P}_0(-L/2) \\ &= \left[\frac{G(\Gamma) + p_0 \gamma_w}{G(\Gamma) p_0 + p_0 \gamma_w} + G(\Gamma) \rho_w (\mathcal{F}_c + \mathcal{F}_{ce}) \right]^{-1}, \end{aligned} \quad (59)$$

where \mathcal{F}_c and \mathcal{F}_{ce} are the following dimensionless factors,

$$\mathcal{F}_c = 1 + \frac{p_1 \tanh(\gamma_c)}{p_0 \gamma_c} > 0, \quad (60)$$

$$\mathcal{F}_{ce} = \frac{1}{G(\Gamma) \rho_e} + \frac{(p_1/p_0) \operatorname{sech}^2(\gamma_c)}{\rho_e (\gamma_e + G(\Gamma)) + \gamma_c \tanh(\gamma_c)} > 0. \quad (61)$$

We note that

$$\mathcal{P}_* = \frac{\rho_e}{\rho_w} (1 - \hat{P}(L/2)),$$

which means that, modulo the differences in diffusivity in the two bulks, a particle is equally likely to (i) go from far away in the west bulk to far away in the east bulk, as it is to (ii) go from far away in the east bulk to far away in the west bulk.

The formula \mathcal{P}_* in (59) is our main result. In the next section, we explore its behavior in various parameter regimes, including showing that it is exact in certain regimes.

4 Flux asymptotics

By the relation in (7), the analysis in section 3 yields the following explicit approximation to the steady-state average flux of particles which enter the channel from far away in the west bulk and ultimately wander far into the east bulk,

$$J_* := (2\pi C_0(\Gamma) a D_w c_\infty) \mathcal{P}_*,$$

where \mathcal{P}_* is the approximate splitting probability in (59). We now explore the asymptotic predictions of this approximate flux formula by analyzing the behavior of \mathcal{P}_* in various parameter regimes.

Recall that \mathcal{P}_* in (59) is a function of six dimensionless parameters. Specifically, \mathcal{P}_* depends on the fraction of time that the gate is open (denoted p_0), the three dimensionless switching rates which compare the switching rate to the timescales of diffusion in the west bulk, channel, and east bulk,

$$\gamma_w = \sqrt{\lambda a^2 / D_w}, \quad \gamma_c = \sqrt{\lambda L^2 / D_c}, \quad \gamma_e = \sqrt{\lambda a^2 / D_e},$$

and the following comparisons of the channel aspect ratio to the change in diffusivity at the west and east channel entrances,

$$\rho_w = \frac{L}{a} \left(\frac{D_w}{D_c} \right)^{\alpha_w}, \quad \rho_e = \frac{L}{a} \left(\frac{D_e}{D_c} \right)^{\alpha_e}.$$

4.1 Slow switching

If the switching rate is much slower than the timescales of diffusion, then

$$\lim_{\max\{\gamma_w, \gamma_e, \gamma_c\} \rightarrow 0} \mathcal{P}_* = p_0 \mathcal{P}_*^{\text{open}},$$

where $\mathcal{P}_*^{\text{open}}$ is the “always open” splitting probability in (24). Hence, the naive estimate that the gated flux is simply p_0 multiplied by the “always open” flux holds for slow switching.

4.2 Fast switching

If the switching rate is much faster than the timescales of diffusion, then

$$\lim_{\min\{\gamma_w, \gamma_e, \gamma_c\} \rightarrow \infty} \mathcal{P}_* = \mathcal{P}_*^{\text{open}},$$

where $\mathcal{P}_*^{\text{open}}$ is in (24). Hence, fast switching is the same as always being open.

4.3 Large ρ_e

In the large $\rho_e = (L/a)(D_e/D_c)^{\alpha_e}$ limit, we have that $\lim_{\rho_e \rightarrow \infty} \mathcal{F}_{ce} = 0$, and therefore,

$$\lim_{\rho_e \rightarrow \infty} \mathcal{P}_* = \left[\frac{G(\Gamma) + p_0 \gamma_w}{G(\Gamma) p_0 + p_0 \gamma_w} + G(\Gamma) \rho_w \mathcal{F}_c \right]^{-1},$$

which recovers the splitting probability derived in Ref. [22] for the case that particles are absorbed at the right end of the channel. This result is to be expected, since if $\rho_e \gg 1$, then any particle which reaches the east end of the channel will likely not return to the west end of the channel because either the channel is long (i.e. $L/a \gg 1$) and/or the diffusivity is much faster in the east bulk than the channel and any non-Itô multiplicative noise will force the particle out the right end of the channel (i.e. $(D_e/D_c)^{\alpha_e} \gg 1$).

4.4 Large $\min\{\rho_w, \rho_e\}$

If both ρ_w and ρ_e are large, then we claim that the splitting probability has the following exact asymptotic,

$$\begin{aligned} \mathcal{P}(-L/2^-) \sim \mathcal{P}_* &\sim \frac{1}{G(\Gamma) \rho_w \mathcal{F}_c} \\ &= \left[G(\Gamma) \left(1 + \frac{p_1 \tanh(\gamma_c)}{p_0 \gamma_c} \right) \frac{L}{a} \left(\frac{D_w}{D_c} \right)^{\alpha_w} \right]^{-1} \quad \text{as } \min\{\rho_w, \rho_e\} \rightarrow \infty, \end{aligned} \tag{62}$$

where $\mathcal{P}(-L/2^-)$ is the exact splitting probability in (38) (which is, in general, not known explicitly). In other words, the approximation \mathcal{P}_* in (59) is exact if $\min\{\rho_w, \rho_e\} \gg 1$. Since $\rho_w = (L/a)(D_w/D_c)^{\alpha_w}$ and $\rho_e = (L/a)(D_e/D_c)^{\alpha_e}$, we may have that $\min\{\rho_w, \rho_e\} \gg 1$ if the channel is long (i.e. $L/a \gg 1$) and/or the diffusivity is slow in the channel and we have non-Itô interpretations of the multiplicative noise (i.e. $(D_w/D_c)^{\alpha_w} \gg 1$ and $(D_e/D_c)^{\alpha_e} \gg 1$).

The second asymptotic equivalence and the final equality in (62) follow immediately from (59)-(61). The first asymptotic equivalence follows from the strong Markov property and results in Refs. [22, 30]. Before detailing the argument, we sketch the main idea. Specifically, it was shown in Ref. [30] that if $\rho_e \gg 1$, then a particle which starts at the east channel entrance is unlikely to reach the west channel entrance. Therefore, the probability of wandering far into the east bulk starting from the west channel entrance is the same as the probability of merely reaching the east channel entrance from the west channel entrance, and the asymptotic of this probability for $\rho_w \gg 1$ was found in Ref. [22].

More precisely, the strong Markov property implies that

$$\begin{aligned} & \left(\int_{a\Gamma} h(-L/2^-, y, z) \mu(y, z) dy dz \right) \inf_{(y,z) \in a\Gamma, i \in \{0,1\}} P_i(L/2, y, z) \leq \mathcal{P}(-L/2^-) \\ & \leq \left(\int_{a\Gamma} h(-L/2^-, y, z) \mu(y, z) dy dz \right) \sup_{(y,z) \in a\Gamma, i \in \{0,1\}} P_i(L/2, y, z), \end{aligned} \quad (63)$$

where $h(x, y, z)$ is the probability that a particle starting at (x, y, z) will reach the east end of the channel given that the gate is initially in its stationary distribution. In words, (63) says that in order to go far into the east bulk from the west channel entrance, the particle must first reach the east channel entrance (which happens with probability given by the integral of h in (63)), and then the particle must go far into the east bulk from the east channel entrance (which is bounded below and above by the infimum and supremum terms in (63)).

It was shown in Ref. [22] that the integral of h in (63) has the following asymptotic behavior,

$$\int_{a\Gamma} h(-L/2^-, y, z) \mu(y, z) dy dz \sim \frac{1}{G(\Gamma)\rho_w \mathcal{F}_c} \quad \text{as } \rho_w \rightarrow \infty. \quad (64)$$

Furthermore,

$$1 - P_i(L/2, y, z) \leq u(L/2, y, z) \quad \text{for all } (y, z) \in a\Gamma, i \in \{0, 1\},$$

where $u(x, y, z)$ is the probability that a particle starting at (x, y, z) will reach the west end of the channel. It was shown in Ref. [30] that

$$\lim_{\rho_e \rightarrow \infty} u(L/2, y, z) = 0 \quad \text{for all } (y, z) \in a\Gamma,$$

and therefore

$$\lim_{\rho_e \rightarrow \infty} P_i(L/2, y, z) = 1 \quad \text{for all } (y, z) \in a\Gamma, i \in \{0, 1\}. \quad (65)$$

Hence, combining (64) and (65) with (63) and using the squeeze theorem yields

$$\mathcal{P}(-L/2^-) \sim \frac{1}{G(\Gamma)\rho_w\mathcal{F}_c} \quad \text{as } \min\{\rho_w, \rho_e\} \rightarrow \infty,$$

which yields (62).

4.5 Small ρ_w

In the limit that $\rho_w = (L/a)(D_w/D_c)^{\alpha_w}$ is small, we obtain

$$\lim_{\rho_w \rightarrow 0} \mathcal{P}_* = p_0 + \frac{p_1 p_0 \gamma_w}{G(\Gamma) + p_0 \gamma_w} = p_0 \left(\frac{G(\Gamma) + \gamma_w}{G(\Gamma) + p_0 \gamma_w} \right) =: \mathcal{P}_*^{\text{gated } \Gamma}, \quad (66)$$

where the final equality defines $\mathcal{P}_*^{\text{gated } \Gamma}$. We note that (66) is not exact in the sense that for a general $\Gamma \subset \mathbb{R}^2$,

$$\lim_{\rho_w \rightarrow 0} \mathcal{P}(-L/2^-) \neq \mathcal{P}_*^{\text{gated } \Gamma}, \quad (67)$$

where $\mathcal{P}(-L/2^-)$ is the exact splitting probability in (38) (which is not known explicitly).

However, (67) is to be expected. To see this, observe first that $\lim_{\rho_w \rightarrow 0} \mathcal{P}(-L/2^-)$ is the probability that a diffusing particle will hit the west entrance to the channel when the gate is open, since if $\rho_w \rightarrow 0$ and all other parameters are fixed, then any particle which reaches the west entrance to the channel when it is open will enter the channel and not exit at the west end of the channel since $\rho_w \ll \rho_e$, and will therefore eventually wander far away into the east bulk. Hence, $\lim_{\rho_w \rightarrow 0} \mathcal{P}(-L/2^-)$ is the probability that a particle will get absorbed at a stochastically gated target with shape Γ , which is notoriously difficult to calculate, even if Γ is a disk [36].

Though $\mathcal{P}_*^{\text{gated } \Gamma}$ is not exact in the sense of (67), the stochastic simulations in section 5.1 below show that $\mathcal{P}_*^{\text{gated } \Gamma}$ is a very accurate approximation of $\lim_{\rho_w \rightarrow 0} \mathcal{P}(-L/2^-)$, at least in the case that Γ is a disk (Figure 3A) or Γ is a square (Figure 3B).

4.6 Short channel

To understand the behavior of \mathcal{P}_* in the case that the channel is short (i.e. $L/a \ll 1$), we introduce a small dimensionless parameter $0 < \varepsilon \ll 1$ and set

$$\rho_w = \varepsilon(D_w/D_c)^{\alpha_w}, \quad \rho_e = \varepsilon(D_e/D_c)^{\alpha_e},$$

and suppose $\gamma_c = \sqrt{\lambda L^2/D_c} = \mathcal{O}(\varepsilon)$ as $\varepsilon \rightarrow 0$. In this case,

$$\lim_{\varepsilon \rightarrow 0} \mathcal{P}_* = \frac{(D_e/D_c)^{\alpha_e}}{(D_w/D_c)^{\alpha_w} + (D_e/D_c)^{\alpha_e}} \mathcal{P}_*^{\text{gated } \Gamma}, \quad (68)$$

where $\mathcal{P}_*^{\text{gated } \Gamma}$ is defined in (66).

The result (68) is intuitive because in order to wander far away into the east bulk, the particle must first reach the west entrance to the channel when it is open (which occurs with approximate probability $\mathcal{P}_*^{\text{gated } \Gamma}$, see section 4.5 above) and then the particle must wander far away into the east bulk rather than the west bulk. If $D_w = D_e$ and $\alpha_w = \alpha_e$ or $\alpha_w = \alpha_e = 0$, then the prefactor in (68) is $1/2$, which accords with symmetry. If $(D_e/D_c)^{\alpha_e} > (D_w/D_c)^{\alpha_w}$, then the prefactor is larger than $1/2$, which reflects the bias for the particle to wander into the east bulk (owing to the spurious force induced by any non-Itô convention [32]).

4.7 Fast and slow switching in bulks versus channel

The fact that there are three diffusivities (D_w , D_c , and D_e) and two lengthscales (L and a) means that the effective switching rates can be very different in the west bulk versus the channel versus the east bulk. For example, it is possible to have

$$\gamma_i \ll \gamma_j \ll \gamma_k,$$

for any permutation of the subscripts i, j, k in $\{w, c, e\}$.

To investigate some of these cases, suppose that the two bulks have identical diffusivity $D_w = D_e = D_b$ and $\alpha_w = \alpha_e = \alpha$ so that $\gamma_w = \gamma_e = \gamma_b := \sqrt{\lambda a^2 / D_b}$ and $\rho_w = \rho_e = \rho := (L/a)(D_b/D_c)^\alpha$. In the limit that the effective bulk switching rate is slow and the effective channel switching rate is fast, we have that

$$\lim_{\gamma_b \rightarrow 0, \gamma_c \rightarrow \infty} \mathcal{P}_* = \frac{p_0}{1 + p_0 + p_0 G(\Gamma) \rho}. \quad (69)$$

In the limit that the effective bulk switching rate is fast and the effective channel switching rate is slow, we have that

$$\lim_{\gamma_b \rightarrow \infty, \gamma_c \rightarrow 0} \mathcal{P}_* = \frac{p_0}{2p_0 + G(\Gamma) \rho}. \quad (70)$$

Interestingly, (69)-(70) imply the following ordering for small ρ ,

$$\lim_{\gamma_b \rightarrow 0, \gamma_c \rightarrow \infty} \mathcal{P}_* < \lim_{\gamma_b \rightarrow \infty, \gamma_c \rightarrow 0} \mathcal{P}_* \quad \text{if } \rho < 1/G(\Gamma),$$

whereas the reverse holds for large ρ ,

$$\lim_{\gamma_b \rightarrow 0, \gamma_c \rightarrow \infty} \mathcal{P}_* > \lim_{\gamma_b \rightarrow \infty, \gamma_c \rightarrow 0} \mathcal{P}_* \quad \text{if } \rho > 1/G(\Gamma).$$

This result is illustrated in Figure 2, where we plot the limiting expressions in (69)-(70) as a function of ρ for the case that $p_0 = 1\%$ and Γ is a disk.

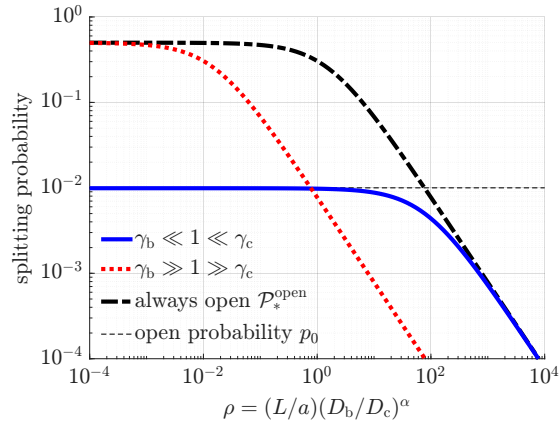


Figure 2: Comparison of the limiting splitting probabilities in (69)-(70).

5 Stochastic simulations

We now compare the approximate splitting probability \mathcal{P}_* in (59) to stochastic simulations in the case that the two bulks have identical diffusivity $D_w = D_e = D_b$ and $\alpha_w = \alpha_e = \alpha$ so that $\gamma_w = \gamma_e = \gamma_b = \sqrt{\lambda a^2 / D_b}$. The simulation algorithms are described in Appendix A.

5.1 Short channel limit

In the short channel limit, we have that

$$\lim_{L \rightarrow 0} \mathcal{P}_* = \frac{p_0}{2} \left(\frac{G(\Gamma) + \gamma_b}{G(\Gamma) + p_0 \gamma_b} \right) = \frac{\mathcal{P}_*^{\text{gated } \Gamma}}{2}, \quad (71)$$

where $\mathcal{P}_*^{\text{gated } \Gamma}$ is (66). In Figure 3, we plot the formula in (71) as a function of γ_b for different values of the open probability p_0 (curves), which compares favorably to stochastic simulations (markers). Indeed, Figure 3 shows that \mathcal{P}_* is an accurate approximation (though not exact) in the regime of (71). Figure 3A is for the case that Γ is the unit disk, and thus $G(\Gamma) = 4/\pi$. Figure 3B is for the case that Γ is the unit square, and thus $G(\Gamma) = 2\pi C_0(\Gamma)/|\Gamma| \approx 2.31$ since the electrostatic capacitance of the unit square is $C_0(\Gamma) \approx 0.367$ [29].

5.2 Variable channel length

Figure 4 plots \mathcal{P}_* as a function of $\rho = (L/a)(D_b/D_c)^\alpha$ for different values of the switching rate λ (different panels) and the open probability p_0 . This figure shows that the approximation agrees well with the stochastic simulations (markers). The channel is cylindrical in this plot (i.e. Γ is the unit disk and $G(\Gamma) = 4/\pi$).

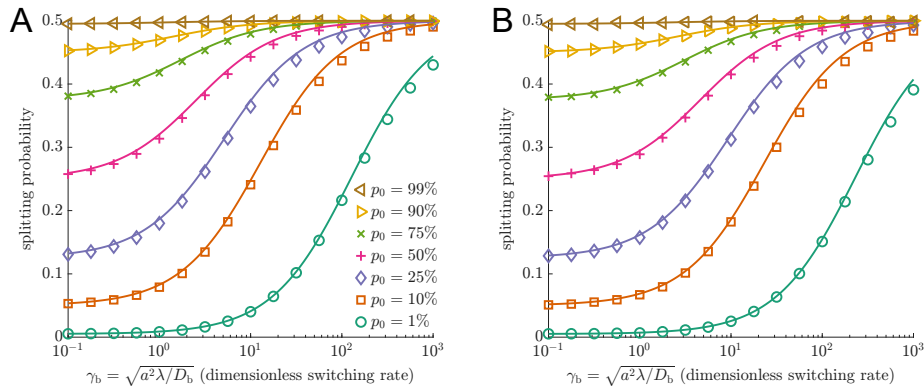


Figure 3: Comparison of the short channel formula in (71) (curves) to stochastic simulation (markers) for different values of the open probability p_0 . In Panel A, Γ is the unit disk. In Panel B, Γ is the unit square.

6 Discussion

In this paper, we used partial differential equation analysis to estimate the average diffusive flux through a channel. Our explicit flux estimate accounts for stochastic gating, channel geometry, and differing diffusivity inside versus outside the channel. We showed that our flux estimate is exact in some parameter regimes, and we used stochastic simulations to show that it remains accurate across other parameter regimes.

Perhaps the first mathematical analysis of the diffusive flux through a stochastically gated channel is the student thesis [18] published later in [20]. Refs. [18, 20] were motivated by insect respiration, in which the flow of oxygen and carbon dioxide through tracheal tubes is modulated by a rapidly opening and closing gate called a spiracle [41]. The mathematical methods developed in Refs. [18, 20] were used to explain certain aspects of the discontinuous gas exchange cycle in insects [21, 25]. Alternative mathematical approaches to the flux through a stochastic gate were developed in several other works [8, 19], including Ref. [9] which accounted for branching channels (motivated by the branched structure of insect tracheae), Ref. [24] which used the Nernst–Planck equation to model the movement of ions in response to a concentration gradient and an electric field, and Ref. [11] which considered non-Markovian gating.

We conclude by comparing our flux estimate to an estimate derived in Ref. [1] and studied in Refs. [2, 3]. Specifically, the following flux estimate was posited in Ref. [1] for the case of a cylindrical channel between two bulks with identical diffusivities $D_w = D_e = D_b$, (see Equation (3.4) in Ref. 1),

$$J_{2017} = \frac{4aD_b c_\infty}{2 + \nu + \frac{p_1}{p_0} \frac{2\gamma_c \nu + (\gamma_c^2 + \nu^2) \tanh(\gamma_c)}{\gamma_c(\nu + \gamma_c \tanh(\gamma_c))}}, \quad \text{where } \nu = \frac{4}{\pi} \frac{L}{a} \frac{D_b}{D_c}. \quad (72)$$

One discrepancy between J_{2017} in (72) and our estimate J_* in (4) is that J_{2017}

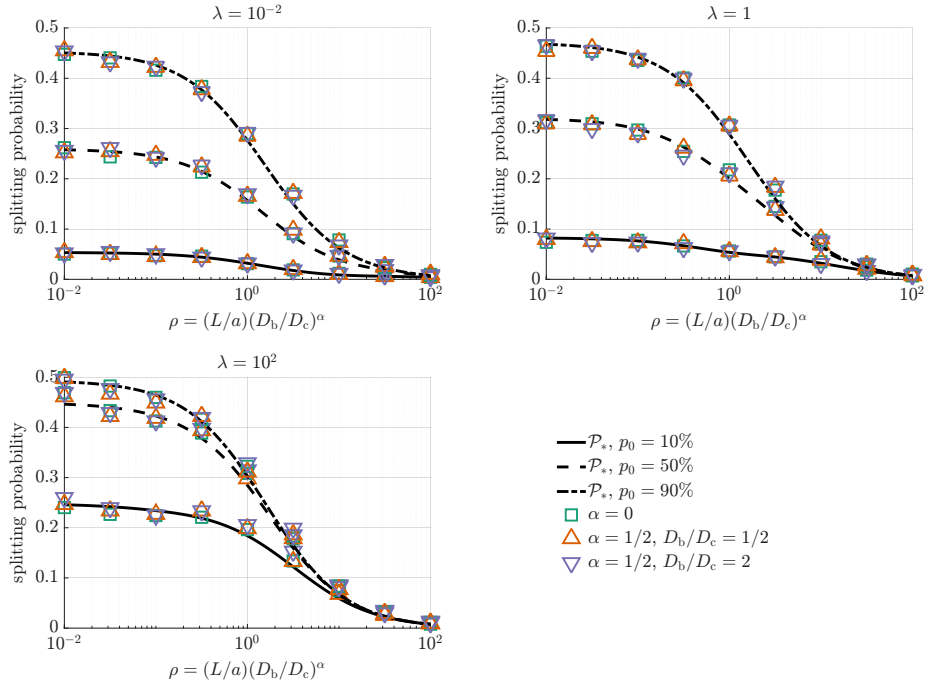


Figure 4: Comparison of \mathcal{P}_* in (59) (black curves) to stochastic simulations (markers).

does not depend on the multiplicative noise convention (i.e. there is no α in J_{2017}). This discrepancy stems from the derivation of J_{2017} which employed a certain effective escape rate from a channel [7] which was recently shown to be valid for $\alpha = 1$ or $D_b = D_c$ [23].

However, significant discrepancies between J_{2017} and J_* persist even if we set $\alpha = 1$ in J_* or take $D_b = D_c$. For example, J_{2017} does not approach the “always open” flux for fast gating,

$$\lim_{\lambda \rightarrow \infty} J_{2017} \neq \lim_{p_0 \rightarrow 1} J_{2017},$$

which contrasts J_* ,

$$\lim_{\lambda \rightarrow \infty} J_* = \lim_{p_0 \rightarrow 1} J_*.$$

Furthermore, J_* is independent of λ if the channel is short,

$$\lim_{L \rightarrow 0} J_{2017} = 4aD_b c_\infty \left(\frac{p_0}{2} \right), \quad (73)$$

which contrasts J_* ,

$$\lim_{L \rightarrow 0} J_* = 4aD_b c_\infty \left(\frac{p_0}{2} \right) \left(\frac{4/\pi + \gamma_b}{4/\pi + p_0 \gamma_b} \right), \quad \text{where } \gamma_b = \sqrt{\lambda a^2 / D_b}. \quad (74)$$

The predictions in (73)-(74) differ sharply if switching is fast compared to the timescale of diffusion in the bulk. Indeed,

$$\lim_{\gamma_b \rightarrow \infty} \left(\frac{\lim_{L \rightarrow 0} J_{2017}}{\lim_{L \rightarrow 0} J_*} \right) = p_0,$$

which predicts that J_{2017} underestimates the actual flux. The accuracy of (74) is supported by Figure 3A.

Acknowledgments

The author gratefully acknowledges support from the National Science Foundation (NSF DMS-2325258).

Data availability

The data that support the findings of this study are available from the corresponding author upon reasonable request.

A Stochastic simulation algorithms

A.1 Short channel simulation algorithm

We start by describing the stochastic simulation algorithm used to produce the markers in Figure 3. Each marker in Figure 3A is computed from 5×10^6 independent simulations, and each marker in Figure 3B is computed from 8×10^5 independent simulations

Owing to symmetry, the simulations in section 5.1 require merely (1) calculating the probability that a particle which reaches the west channel entrance from far away in the west bulk will eventually hit this west channel entrance when the gate is open and (2) multiplying this probability by 1/2. For the case that the channel cross-section is a disk (i.e. Figure 3A), the simulation of (1) follows a simulation algorithm used in Ref. [22]. For the case that the channel cross-section is a square (i.e. Figure 3B), we follow the following modification of that simulation algorithm.

Step 0. Initialize the gate to be open with probability p_0 and closed with probability $p_1 = 1 - p_0$. If the gate is initially open, then the particle is absorbed and the simulation ends. If the gate is initially closed, then we must initialize the particle to be at a random position on the unit square,

$$\mathbf{X}(0) = (0, Y(0), Z(0)) \in \{0\} \times [-1/2, 1/2]^2, \quad (75)$$

where the distribution of $(Y(0), Z(0))$ is the harmonic measure μ in (39)-(40). While μ is known explicitly if Γ is a disk (see (13)), we do not know an explicit formula for μ if Γ is a square. Nevertheless, one can approximate samples of μ on

the square Γ by first letting (X', Y', Z') be uniformly distributed on any sphere containing the unit disk, and then following the algorithm of Bernoff, Lindsay, and Schmidt [6] until the particle either (i) reaches Γ or (ii) reaches a large distance $R_\infty = 10^{10}$ from the origin. If (i) happens, then the resulting position on the square gives (75). If (ii) happens, then we repeat until (i) happens.

Proceed to Step 1.

Step 1. Given the particle $\mathbf{X}_0 = (0, Y_0, Z_0) \in \Gamma$ and given that the gate is closed, we sample a realization of the waiting time until the gate opens, which is given exactly by the following exponential random variable with mean $1/\lambda_1$,

$$\tau = E/\lambda_1,$$

where E is a unit mean exponential random variable. Before time τ elapses, the particle diffuses in three dimensions with a reflecting boundary condition at $x = 0$, and hence its position when the gate opens is given exactly by

$$X = -|0 + \sqrt{2D_b\tau}\mathcal{N}_x|, \quad (76)$$

$$Y = Y_0 + \sqrt{2D_b\tau}\mathcal{N}_y, \quad (77)$$

$$Z = Z_0 + \sqrt{2D_b\tau}\mathcal{N}_z, \quad (78)$$

where $\mathcal{N}_x, \mathcal{N}_y, \mathcal{N}_z$, are independent standard normal random variables.

Step 2: Starting from $\mathbf{X} = (X, Y, Z)$ in (76)-(78), we follow the algorithm in Ref. 6 to simulate the particle trajectory until the particle either (i) reaches a distance $R_\infty = 10^{10} \gg 1$ from the west channel entrance or (ii) hits the west channel entrance. If (i) occurs, then we assume that the particle will never return to the channel and the simulation ends. If (ii) occurs, then we set the gate to be closed with probability

$$p_1(1 - e^{-(\lambda_0 + \lambda_1)t}), \quad (79)$$

where t is the time elapsed since the start of Step 2. If the gate is open, then the particle is absorbed and the simulation ends. If the gate is closed, then return to Step 1.

A.2 Variable channel length simulations

We now describe the simulation algorithm used to produce the markers in Figure 4. Each marker in Figure 4 is computed from 8×10^3 independent simulations.

Step 1. Follow a simulation algorithm used in Ref. [22] to simulate the particle until it either (i) wanders a large distance $R_\infty = 10^{10}$ away from the channel in the west bulk or (ii) reaches the east channel entrance. If (i) happens, then it is assumed that the particle will never wander far away into the east bulk and the simulation ends. If (ii) happens, then proceed to Step 2.

Step 2. Follow a simulation algorithm used in Ref. [22] to simulate the particle until it either (i) wanders a large distance $R_\infty = 10^{10}$ away from the

channel in the east bulk or (ii) reaches the west channel entrance (where the gate is). If (i) happens, then it is assumed that the particle has wandered far away into the east bulk and will never return to the west bulk and the simulation ends. If (ii) happens, then return to Step 1.

References

- [1] A. Berezhkovskii and S. Bezrukov. Effect of stochastic gating on channel-facilitated transport of non-interacting and strongly repelling solutes. *The Journal of Chemical Physics*, 147(8):084109, 2017.
- [2] A. Berezhkovskii and S. Bezrukov. Effect of stochastic gating on the flux through a membrane channel: A steady-state approach. *Journal of Physics: Condensed Matter*, 30(25):254006, 2018.
- [3] A. Berezhkovskii and S. Bezrukov. Stochastic gating as a novel mechanism for channel selectivity. *Biophysical Journal*, 114(5):1026–1029, 2018.
- [4] A. Berezhkovskii and S. Shvartsman. Diffusive flux in a model of stochastically gated oxygen transport in insect respiration. *The Journal of Chemical Physics*, 144(20):204101, 2016.
- [5] H. Berg and E. Purcell. Physics of chemoreception. *Biophys J*, 20(2):193–219, 1977.
- [6] A. Bernoff, A. Lindsay, and D. Schmidt. Boundary Homogenization and Capture Time Distributions of Semipermeable Membranes with Periodic Patterns of Reactive Sites. *Multiscale Modeling & Simulation*, 16(3):1411–1447, Jan. 2018.
- [7] S. Bezrukov, A. Berezhkovskii, M. Pustovoit, and A. Szabo. Particle number fluctuations in a membrane channel. *The Journal of Chemical Physics*, 113(18):8206–8211, 2000.
- [8] P. Bressloff and S. Lawley. Moment equations for a piecewise deterministic PDE. *J Phys A*, 48(10):105001, 2015.
- [9] P. Bressloff and S. Lawley. Diffusion on a tree with stochastically gated nodes. *J Phys A*, 49(24):245601, 2016.
- [10] P. Bressloff and S. Lawley. Temporal disorder as a mechanism for spatially heterogeneous diffusion. *Phys Rev E - Rapid Comm*, 95(6):060101, 2017.
- [11] P. C. Bressloff, S. D. Lawley, and P. Murphy. Diffusion in an age-structured randomly switching environment. *Journal of Physics A: Mathematical and Theoretical*, 51(31):315001, Aug. 2018.
- [12] D. Grebenkov. Analytical representations of the spread harmonic measure density. *Physical Review E*, 91(5):052108, 2015.

- [13] P. Hänggi and H. Thomas. Stochastic processes: Time evolution, symmetries and linear response. *Physics Reports*, 88(4):207–319, 1982.
- [14] M. Häusser. The Hodgkin-Huxley theory of the action potential. *Nature neuroscience*, 3:1165–1165, 2000.
- [15] A. Hodgkin and A. Huxley. A quantitative description of membrane current and its application to conduction and excitation in nerve. *The Journal of Physiology*, 117(4):500–544, 1952.
- [16] K. Itô. Stochastic integral. *Proceedings of the Imperial Academy*, 20(8):519–524, 1944.
- [17] T. Kozai, J. Fernandez-Martinez, L. E. Kapinos, P. Gallardo, T. Van Eeuwen, M. Saladin, R. Eliasian, A. Mazur, W. Zhang, J. Tempkin, et al. Karyopherins remodel the dynamic organization of the nuclear pore complex transport barrier. *Nature Cell Biology*, pages 1–13, 2025.
- [18] S. Lawley. *Stochastic Switching in Evolution Equations*. PhD thesis, Duke University, 2014.
- [19] S. Lawley. Boundary value problems for statistics of diffusion in a randomly switching environment: PDE and SDE perspectives. *SIAM J Appl Dyn Syst*, 15, 2016.
- [20] S. Lawley, J. C. Mattingly, and M. C. Reed. Stochastic switching in infinite dimensions with applications to random parabolic PDE. *SIAM J Math Anal*, 47(4):3035–3063, 2015.
- [21] S. Lawley, H. Nijhout, and M. Reed. Spiracular fluttering decouples oxygen uptake and water loss: a stochastic PDE model of respiratory water loss in insects. *Journal of Mathematical Biology*, 84(6):40, 2022.
- [22] S. D. Lawley. Diffusive flux into a stochastically gated tube. *arXiv preprint arXiv:2603.09841*, 2026.
- [23] S. D. Lawley. Escape from a channel. *The Journal of Chemical Physics*, 164(6):064116, 2026.
- [24] S. D. Lawley and J. P. Keener. Electrodiffusive flux through a stochastically gated ion channel. *SIAM Journal on Applied Mathematics*, 79(2):551–571, 2019.
- [25] S. D. Lawley, M. C. Reed, and H. F. Nijhout. Spiracular fluttering increases oxygen uptake. *PLoS One*, 15(5):e0232450, 2020.
- [26] R. Mannella and P. McClintock. Itô versus stratonovich: 30 years later. *Fluctuation and Noise Letters*, 11(01):1240010, 2012.
- [27] R. Phillips, J. Kondev, J. Theriot, and H. Garcia. *Physical biology of the cell*. Garland Science, 2012.

- [28] M. Piccolino. Fifty years of the Hodgkin-Huxley era. *TRENDS in Neurosciences*, 25(11):552–553, 2002.
- [29] F. H. Read. Improved extrapolation technique in the boundary element method to find the capacitances of the unit square and cube. *Journal of Computational Physics*, 133(1):1–5, 1997.
- [30] V. Richardson, Y. H. Ling, and S. D. Lawley. Yet another look at narrow escape through a tube. *arXiv preprint arXiv:2602.21396*, 2026.
- [31] T. Rostovtseva and M. Colombini. VDAC channels mediate and gate the flow of ATP: implications for the regulation of mitochondrial function. *Biophysical journal*, 72(5):1954–1962, 1997.
- [32] A. S. Serov, F. Laurent, C. Floderer, K. Perronet, C. Favard, D. Muriiaux, N. Westbrook, C. L. Vestergaard, and J.-B. Masson. Statistical tests for force inference in heterogeneous environments. *Scientific reports*, 10(1):3783, 2020.
- [33] I. Sneddon. *Mixed boundary value problems in potential theory*. North-Holland Publishing Company, Amsterdam, 1966.
- [34] I. Sokolov. Ito, Stratonovich, Hänggi and all the rest: The thermodynamics of interpretation. *Chemical Physics*, 375(2-3):359–363, 2010.
- [35] R. Stratonovich. A new representation for stochastic integrals and equations. *SIAM Journal on Control*, 4(2):362–371, 1966.
- [36] A. Szabo, D. Shoup, S. H. Northrup, and J. A. McCammon. Stochastically gated diffusion-influenced reactions. *J. Chem. Phys*, 77(9):4484–4493, 1982.
- [37] H.-R. Tung and S. D. Lawley. Escape from heterogeneous diffusion. *arXiv preprint arXiv:2512.19646*, 2025.
- [38] H.-R. Tung and S. D. Lawley. Stochastic search with space-dependent diffusivity. *arXiv preprint arXiv:2601.08740*, 2026.
- [39] G. Vaccario, C. Antoine, and J. Talbot. First-passage times in d -dimensional heterogeneous media. *Phys Rev Lett*, 115(24):240601, 2015.
- [40] N. Van Kampen. Itô versus stratonovich. *Journal of Statistical Physics*, 24(1):175–187, 1981.
- [41] V. B. Wigglesworth. The respiration of insects. *Biol. Rev.*, 6(2):181–220, 1931.